Electronic Supplementary Material (ESI) for Nanoscale Advances.

Supporting information

Label-free sensing below the sub-diffraction limit of virus-like particles by wide-field photon state parametric imaging of a gold nanodot array

Xiao Jin,[1] Heng Zhang, [1] Bin Ni,[1] Weiping Liu,[1] Lianping Hou,[2] John H. Marsh,[2] Shengwei Ye,[2] Xiao Sun,[2] Xiaofeng Li,[3] Shanhu Li,[4] Lei Dong,[5] Jamie Jiangmin Hou, [6] Ming Sun,[1] Bin Xu,[1] Jichuan Xiong,[1,*], and Xuefeng Liu,[1, *]

[1]School of Electronic and Optical Engineering, Nanjing University of Science and Technology, Nanjing 210094, P. R. China
[2]James Watt School of Engineering, University of Glasgow, Glasgow, G12 8QQ, UK
[3]State Key Laboratory of Respiratory Disease, National Clinical Research Center for Respiratory Disease, Guangzhou Institute of Respiratory Disease,
the First Affiliated Hospital of Guangzhou Medical University, Guangzhou Medical University, Guangzhou 510182, P. R. China
[4]Department of Cell Engineering, Beijing Institute of Biotechnology, Beijing, 100850, P. R. China
[5]School of Life Science, Beijing Institute of Technology, Beijing 100081, P. R. China
[6]The Royal College of Surgeons of Edinburgh, Nicolson Street, Edinburgh, Scotland, UK EH8 9DW

X. Jin and H. Zhang contributed equally to the manuscript

***Corresponding author:** jichuan.xiong@njust.edu.cn and liuxf_1956@sina.com

This PDF file includes:

I. Calculation of PIMI images

The PIMI images ($sin\delta$ and ϕ) can be obtained by the following measurement procedure:
Using the LCPR, the polarization angle of the illumination was modulated precisely from 0° through 360° in steps of 18°, the far-field scattering images under each illumination condition were recorded. The intensity variation of the recorded image pixels corresponding to each object point can be represented by the equation:

$$I_i = \frac{1}{2} I_0 \left[1 + \sin\delta \sin 2(\theta_i - \phi)\right]. \tag{S1}$$

where I_i (the subscript i indicates the number of polarization rotation angles) is the pixel intensity. I_0 represents the average intensity under all polarization states. $\sin\delta$ is the sine of the phase difference between two orthogonal polarization components of the scattered light. θ_i is the polarization angle of the linearly polarized incident beam and ϕ is the polarization ellipse orientation angle of the beam reflected from the sample.
By expanding Eq. (S1) trigonometrically, it can be reformulated in the following form:

$$I_i = a_0 + a_1 sin2\theta_i + a_2 cos2\theta_i \tag{S2}$$

$$a_0 = \frac{1}{2} I_0,\ a_1 = \frac{1}{2} I_0 sin\delta cos2\phi,\ a_2 = -\frac{1}{2} I_0 sin\delta sin2\phi. \tag{S3}$$

Through precise control of the LCPR, the incident polarization angle θ_i can be modulated from zero to 360 degrees, with a total number of steps $N = 360°/18°$, from this, a_0, a_1 and a_2 can be calculated as:

$$a_0 = \sum_{i=1}^{N} \frac{1}{N} I_i,\ a_1 = \sum_{i=1}^{N} \frac{2}{N} I_i sin\alpha_i,\ a_2 = \sum_{i=1}^{N} \frac{2}{N} I_i cos\alpha_i. \tag{S4}$$

Thus, the PIMI parameters, $sin\delta$ and ϕ can be extracted by utilizing the above equations.

$$sin\delta = \frac{\sqrt{a_1^2 + a_2^2}}{a_0},\ \phi = \frac{1}{2} arccos\left(\frac{a_1}{\sqrt{a_1^2 + a_2^2}}\right). \tag{S5}$$

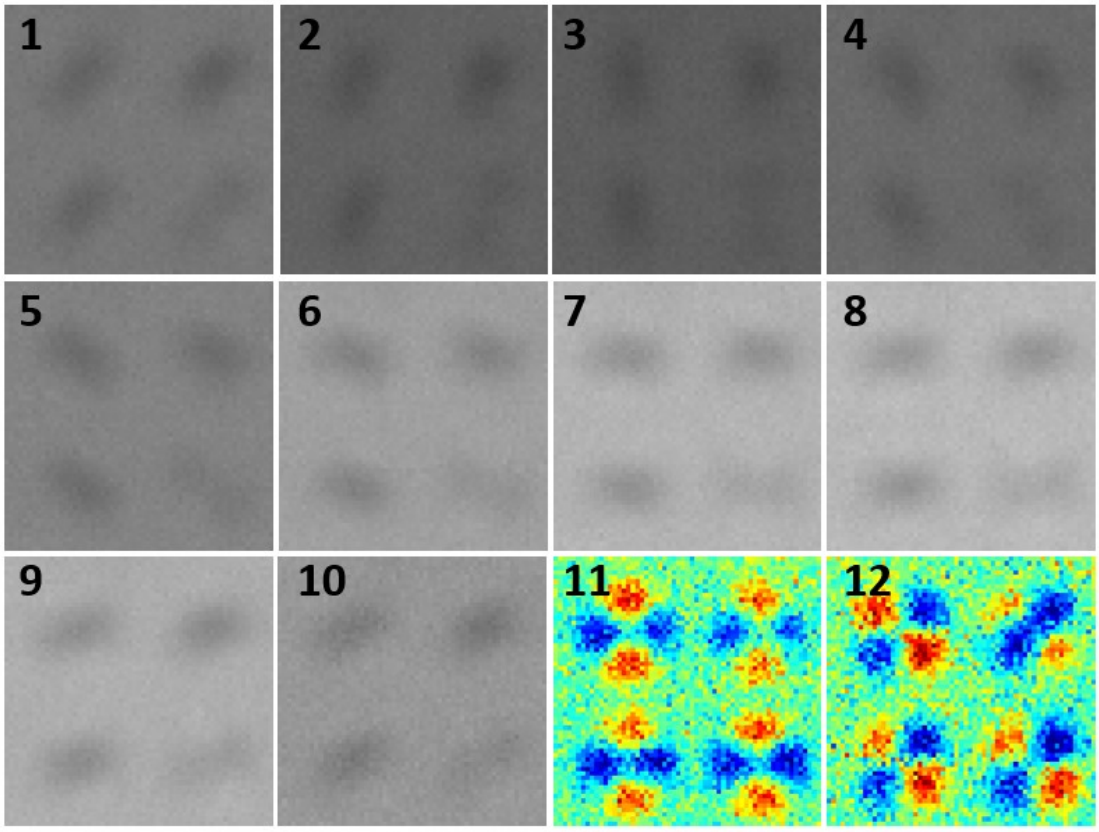

Fig. S1 1-10: 10 PIMI initial images of gold nanodots under a rotating illumination with a step of 18°,
11: PIMI sinδ image, 12: PIMI ϕ image

II. The fabrication process of gold nanodot array

The device of gold nanodot array was realized by following fabrication processes. A silicon sample was first cleaned by acetone and Isopropyl Alcohol (IPA) solvents separately. These two steps were carried out in a water bath at a temperature of 50 °C. Then, ultrasonic cleaning was applied for better cleaning effects at room temperature. After the above cleaning processes, a 200 nm thick layer Polymethyl Methacrylate (PMMA) photoresist was spun on the surface of the silicon sample by controlling the spinning speed. Electron beam lithography (EBL) was used to define the gold nanodot array pattern on the PMMA resist with a high resolution. After development, the gold nanodot array pattern was transferred to PMMA. Next, a 10 nm thick titanium layer and a 70 nm thick gold layer were deposited successively on the surface of the silicon sample by the Electron Beam Evaporation method. The 10 nm thick titanium was first deposited mainly to enhance the metal adhesion with the silicon surface. After a standard lift-off process, the gold nanodot array was finally realized. Here, the gold nanodots were designed with a diameter of 110 nm.

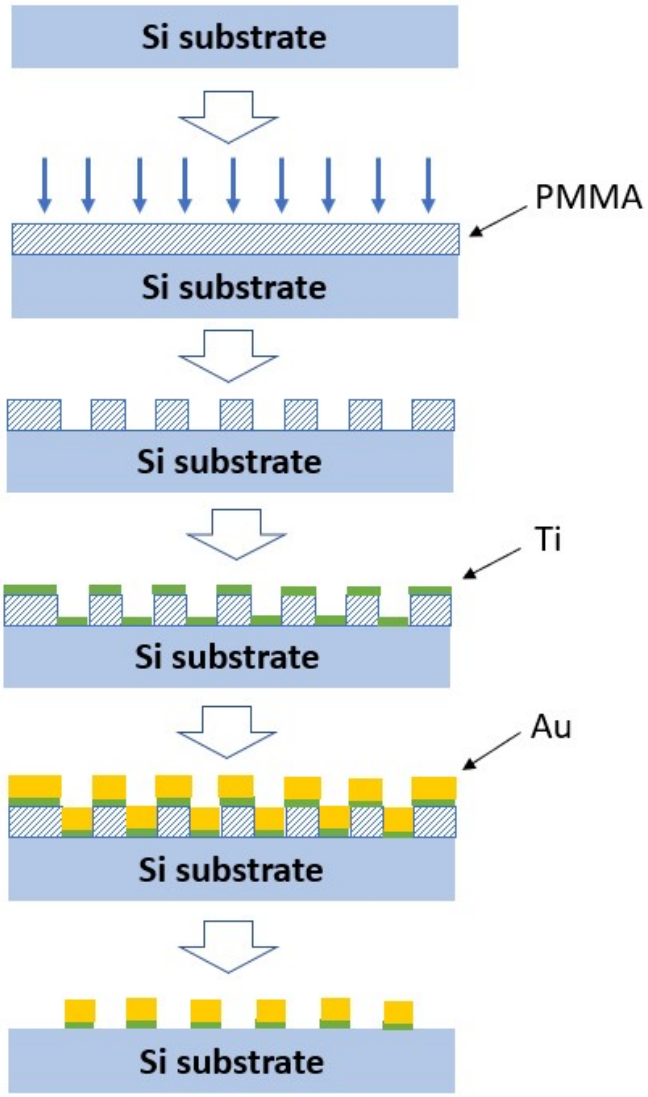

Fig. S2 Fabrication processes of gold nanodot array

III. Large scale images of gold nanodots at intervals of 0.5 μm and 1 μm

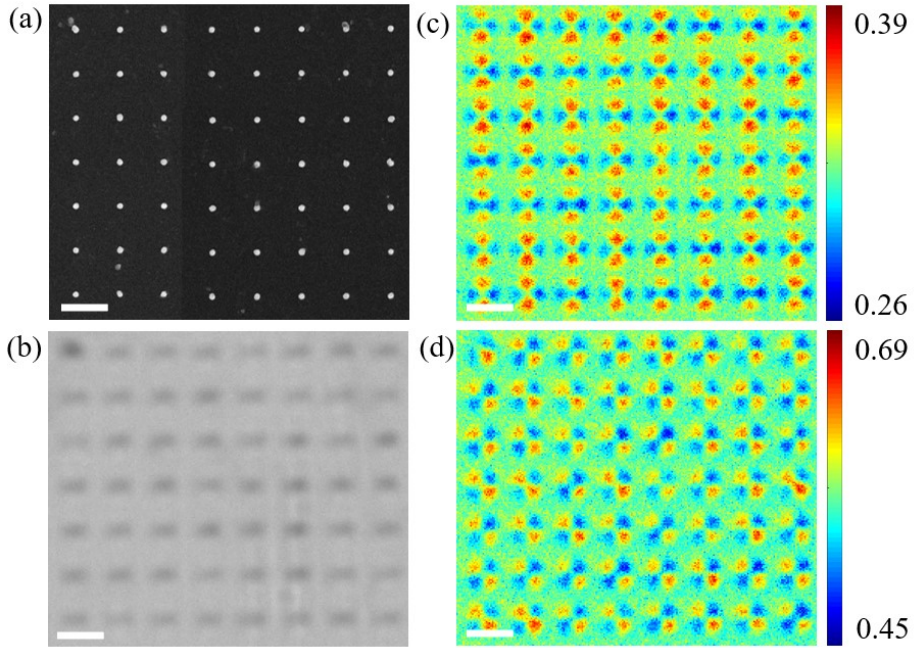

Fig. S3 Large scale images from (a)SEM, (b)conventional microscopy (c)PIMI sinδ and (d)PIMI ϕ at the same area on the array with 1μm interval between two gold nanodots. Scale bar: 1μm.

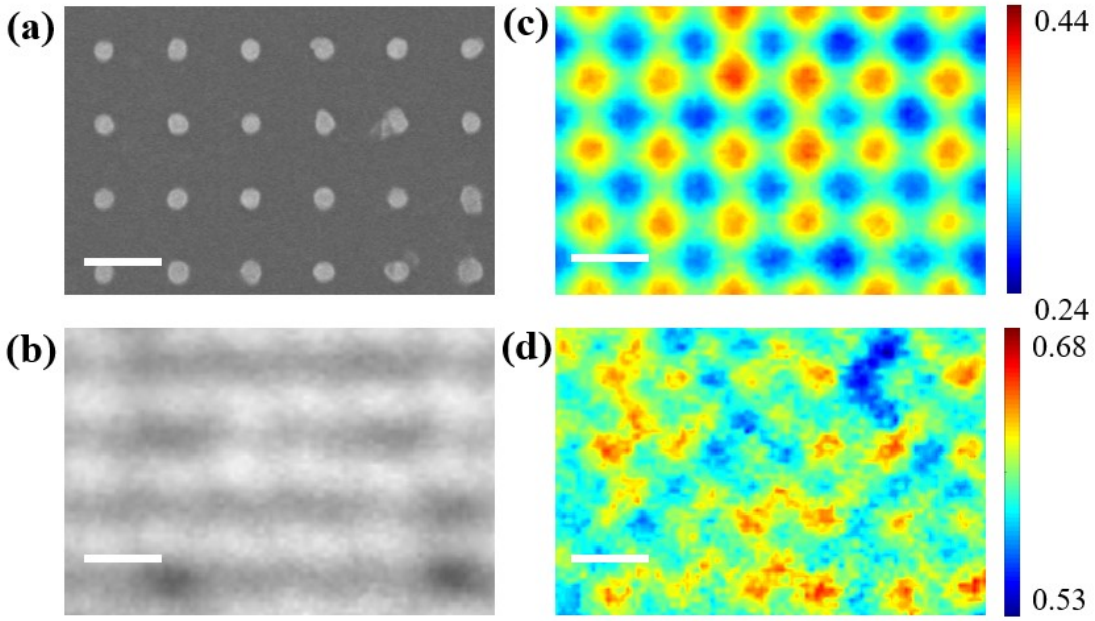

Fig. S4 Large scale images from (a)SEM, (b)conventional microscopy (c)PIMI sinδ and (d)PIMI ϕ at the same area on the array with 0.5μm interval between two gold nanodots. Scale bar: 0.5μm.

IV. Calculation of detecting area and limit of detecting concentration of virus

A series of simulations with different distances has been implemented, as shown in Fig. 1. The interval of gold nanodots is 1μm.

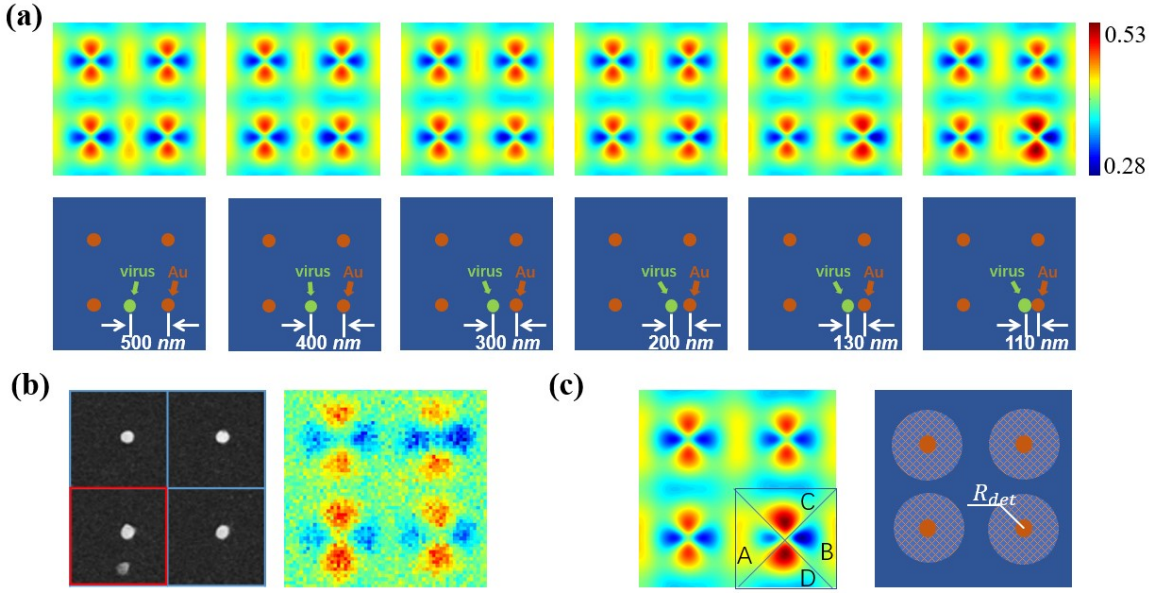

Fig. S5 (a) simulated PIMI sinδ with different distances between the gold nanodot and virus. (b) SEM and sinδ images for a virus with a distance of about 400 nm. (c) the calculation for the radius of the detecting area.

When the virus lay in the middle position between the gold nanodots, the distance is too far to generate periodicity breaking, and the four dipoles share a similar shape. As the virus gets close to the lower right gold nanodot, its shape starts to deform. In the rightmost figures, the virus was directly attached to the gold nanodot, which generates a transverse asymmetric photon state distribution. From Fig. S5(b), we can also observe a virus that is around 400 nm from the adjacent gold nanodot. The virus does not impact on the periodicity of photon state distribution.

Since the large distance between the virus and gold nanodots confer an invalid influence, there is a need to define the effective detecting area. As shown in Fig. S5(c), the method to describe aperiodicity in the article could also be used. The dipole is divided to four parts, and the aperiodicity of sinδ are calculated at every distance. When the asymmetry reaches half of the maximum value (0.5388) in the experiment, the present distance between the virus and the gold nanodot is defined as the radius of the detecting area R_{det}. That means the virus falls within the circle with a radius R_{det} respect to the center gold nanodot will always generate a reaction to broken periodicity and lead to the change of photon state distribution. By constantly changing the distance and checking the aperiodicity, the rough calculated value for R_{det} is 150 nm.

To evaluate the detection ability of nanodots array, we could calculate the single virus detecting process and set the sample volume as 150 μL, which is a normal value in practice. When a virus falls into the array, there will be a probability P that the virus could be detected. P is related to the detecting area, which is shown in Fig. S5(C). We could assume that this virus has an equal possibility to locate at any point in the array, then P should be the ratio of detecting areas to the whole areas (In practice, this ratio will be higher, because of the higher adsorption between nanodots and viruses when depositing).

$$P = \frac{\pi {R_{det}}^2}{L^2} \tag{S6}$$

Here R_{det} is the radius of the detecting area, L is the interval for the gold array.

After a series of N viruses drop onto the surface, the detecting probability for N viruses could be treated as N-independent events. To calculate the lower limit quantity for virus detecting, a parameter P_N is defined as the possibility of 'At least one virus is detected by the gold array'.

$$P_N = 1 - C_N^0 P^0 (1 - P)^N \tag{S7}$$

We set a threshold $P_N > 0.999$ as the standard for a stable detecting ability, where the solved N is

$$N > \frac{-3}{lg(1 - \frac{\pi {R_{det}}^2}{L^2})} \tag{S8}$$

which can satisfy virus detecting.

When the interval L is 1μm, the minimum N derived from the inequality above is 96, which means the detecting limit of concentration is 96 copies/150μL. When the interval L is 0.5μm, the limit of concentration decreases to 21 copies/150μL.